

HOOK FORMULA FOR SKEW SHAPES

A Paper  
Submitted to the Graduate Faculty  
of the  
North Dakota State University  
of Agriculture and Applied Science

By  
Megan Lisa Jensen

In Partial Fulfillment of the Requirements  
for the Degree of  
MASTER OF SCIENCE

Major Department:  
Mathematics

July 2019

Fargo, North Dakota

# NORTH DAKOTA STATE UNIVERSITY

Graduate School

---

**Title**

HOOK FORMULA FOR SKEW SHAPES

---

**By**

Megan Lisa Jensen

---

The supervisory committee certifies that this paper complies with North Dakota State University's regulations and meets the accepted standards for the degree of

MASTER OF SCIENCE

SUPERVISORY COMMITTEE:

Dr. Jessica Striker

Chair

---

Dr. Benton Duncan

---

Dr. Dogan Comez

---

Dr. Sigurd Johnson

---

Approved:

3 July 2019

Date

---

Dr. Benton Duncan

Department Chair

---

## ABSTRACT

The number of standard Young tableaux is given by the hook-length formula of Frame, Robinson, and Thrall. Recently, Naruse found a hook-length formula for the number of skew shaped standard Young tableaux. In a series of papers, Morales, Pak, and Panova prove the Naruse hook-length formula as well as  $q$ -analogues of Naruse's formula. In this paper, we will discuss their work, including connections between excited diagrams and Dyck paths.

## ACKNOWLEDGEMENTS

I would like to thank my advisor, Dr. Jessica Striker, for directing me towards this fascinating subject and for being so patient with me in writing my paper. Also, thank you to Dylan Heuer and Corey Vorland for proof-reading my paper. I would also like to thank my fellow graduate students, especially my office mates, for always lending me their ears.

## DEDICATION

This expository paper is dedicated to my family. Alex, thank you for believing in me. Without your encouragement and support, I would not have been able to do this. Thank you to my family for always being my cheering section. I love you all.

# TABLE OF CONTENTS

ABSTRACT . . . . .	iii
ACKNOWLEDGEMENTS . . . . .	iv
DEDICATION . . . . .	v
LIST OF FIGURES . . . . .	viii
1. INTRODUCTION . . . . .	1
2. BACKGROUND . . . . .	2
2.1. Definitions and Operations . . . . .	2
3. THE HOOK LENGTH FORMULA . . . . .	8
3.1. History . . . . .	8
3.2. Hook Content Formula . . . . .	9
3.3. $q$ -analogues of the Hook Length Formula and Hook Content Formula . . . . .	9
4. HOOK LENGTH FORMULA FOR SKEW SHAPES . . . . .	11
4.1. Naruse Hook Length Formula . . . . .	11
4.2. Proof of the NHLF Using Excited Diagrams . . . . .	12
4.3. Proof of the NHLF Using Pleasant Diagrams . . . . .	13
4.4. Proof of the NHLF Using Shadow Lines . . . . .	17
5. FUN WITH EXCITED DIAGRAMS . . . . .	19
5.1. Catalan Numbers and Objects . . . . .	19
5.2. Catalan Numbers and Excited Diagrams . . . . .	21
6. OTHER RESULTS . . . . .	30
6.1. Lozenge Tilings and Excited Diagrams . . . . .	30
6.2. Reverse Plane Partitions of Skew Staircase Shapes and $q$ -Euler Numbers . . . . .	32
6.3. Future Investigation . . . . .	33

REFERENCES . . . . . 34

## LIST OF FIGURES

<u>Figure</u>	<u>Page</u>
2.1. Young diagrams of the partitions of 5. . . . .	3
2.2. The skew diagram constructed from $\lambda$ and $\mu$ . . . . .	3
2.3. Hook lengths of a Young diagram. . . . .	3
2.4. Two elements of SYT(5,3,3,2,1). . . . .	4
2.5. Two standard Young tableaux of skew shape. . . . .	4
2.6. Two elements of SSYT(5,3,3,2,1). . . . .	5
2.7. Two plane partitions of shape (3,3,1). . . . .	6
2.8. Two reverse plane partitions of shape (3,3,1). . . . .	6
3.1. The first Young diagram above shows the content of each cell. The second Young diagram shows the values of $m + c(u)$ for each cell. . . . .	9
4.1. The excited diagrams of shape $(5, 3, 3, 2, 1)/(3, 1, 1)$ . . . . .	12
4.2. Hook lengths in the excited diagrams of shape $(5, 3, 3, 2, 1)/(3, 1, 1)$ . . . . .	12
4.3. The pleasant diagrams of shape (2,2). . . . .	14
5.1. Catalan objects. . . . .	20
5.2. Finding the flag of the tableau of shape $(12, 12, 10, 9, 9, 6, 6, 6)/(7, 5, 5, 4, 2)$ . . . . .	23
5.3. Constructing a flagged tableau given an excited diagram. . . . .	23
5.4. Border strips of $\delta_8/\delta_4$ . . . . .	25
5.5. The Kreiman decomposition for $\delta_8/\delta_4$ . . . . .	26
5.6. Boarder strips of $\delta_8/\delta_4$ . . . . .	28
5.7. Kreiman outer decompositions of $\delta_8/\delta_4$ . . . . .	28
6.1. A triangular grid and lozenges. . . . .	30
6.2. Excited diagrams of skew shape $(3, 3, 2)/(2, 1)$ . . . . .	31
6.3. Lozenge tilings corresponding to the excited diagrams of skew shape $(3, 3, 2)/(2, 1)$ . . . . .	31



# 1. INTRODUCTION

Standard Young tableaux are a common mathematical construct in areas such as representation theory, algebraic combinatorics, and enumerative combinatorics. In combinatorics, we appreciate an explicit counting formula whenever it can be found. The number of standard Young tableaux of partition shape  $\lambda$ , denoted  $f^\lambda$ , is determined by the celebrated hook length formula of Frame, Robinson, and Thrall. The product formula, which was found in 1954, is given by  $f^\lambda = \frac{n!}{\prod_{u \in [\lambda]} h(u)}$  (see Chapter 2 for definitions of notation). Stanley related this formula to the Schur symmetric functions as follows:  $s_\lambda(1, q, q^2, \dots) = q^{b(\lambda)} \prod_{u \in [\lambda]} \frac{1}{1 - q^{h(u)}}$ . The first topic of this paper is to explore proofs and generalizations of the hook length formula.

Recently, in 2014, Naruse found a formula that counts the number of standard Young tableaux of skew shape  $\lambda/\mu$  by looking at a new object called excited diagrams,  $\varepsilon(\lambda/\mu)$ . The formula is as follows: for  $\lambda, \mu$  partitions such that  $\mu \subset \lambda$ ,  $f^{\lambda/\mu} = |\lambda/\mu|! \sum_{D \in \varepsilon(\lambda/\mu)} \prod_{u \in D} \frac{1}{h(u)}$ .

In a series of papers [10, 11, 12], Morales, Pak, and Panova give multiple proofs of the Naruse hook length formula. The second topic of this paper is to investigate these proofs and  $q$ -analogues of the Naruse hook length formula.

Finally, we will discuss an interesting corollary that connects Dyck paths, counted by Catalan numbers, with excited diagrams of thick strips.

This paper begins with Chapter 2 containing prerequisite definitions and examples. Then in Chapter 3 we discuss the hook length formula for standard Young tableaux as well as its adaptation for semistandard Young tableaux. Chapter 4 is dedicated to the Naruse hook length formula for skew standard Young tableaux and three different proofs of it. In Chapter 5, we discuss a connection between excited diagrams and Catalan numbers. Chapter 6 contains other findings from [10, 11, 12], related recent work, and future directions of research.

## 2. BACKGROUND

In this chapter, we give background definitions and formulas that are fundamental for understanding the work of Morales, Pak, and Panova [10, 11, 12]. Many of these combinatorial definitions are central to tableaux theory and combinatorics itself.

### 2.1. Definitions and Operations

The structures of Young tableaux were derived from partitions of positive integers. The concept of partitioning integers occurs in mathematics and physics. Below we give the definition of a partition and related ideas, followed by examples.

**Definition 2.1.1.** Given a positive integer  $n$ , we say  $\lambda = (\lambda_1, \dots, \lambda_r)$  is a *partition* of  $n$ , when  $\lambda_1 + \dots + \lambda_r = n$  such that each  $\lambda_i$  is a positive integer and  $\lambda_1 \geq \lambda_2 \geq \dots \geq \lambda_r$ . We say that the *length* of  $\lambda = (\lambda_1, \dots, \lambda_r)$  is  $r$ . That is,  $\ell(\lambda) = r$ . Given a partition  $\lambda = (\lambda_1, \dots, \lambda_r)$  its Young diagram, denoted  $[\lambda]$ , is a collection of boxes, or cells, arranged in left-justified rows with  $\lambda_i$  boxes in the  $i$ -th row. The upper left cell of  $[\lambda]$  is denoted  $(1, 1)$ , and the rest of the cells are denoted with  $(i, j)$  matrix indexing. The number of cells in  $[\lambda]$  is called the *size* of  $[\lambda]$ . We denote this as  $|\lambda| = n$ . The *conjugate partition* of  $\lambda$ , written  $\lambda'$ , is obtained by reflecting  $[\lambda]$  over its main diagonal. After this process, the first row of  $\lambda$  will become the first column of  $\lambda'$  and so on. The *Durfee square*, denoted  $\square^\lambda$ , is the largest subdiagram of  $[\lambda]$  that has the form  $\{(i, j) \mid 1 \leq i \leq \lambda_1, 1 \leq j \leq \ell(\lambda)\}$ . Consider  $\lambda = (\lambda_1, \dots, \lambda_r)$  and  $\mu = (\mu_1, \dots, \mu_s)$ . We say  $[\mu] \subseteq [\lambda]$  if  $\mu_i \leq \lambda_i$ , for all  $i$ . If  $[\mu] \subseteq [\lambda]$ , the *skew shape*  $\lambda/\mu$  is constructed by removing the boxes of  $[\mu]$  from  $[\lambda]$ . We call a box an *inside corner* of the deleted diagram  $\mu$  if the box below and the box to the right of it are both not in  $\mu$ . We call a box an *outside box* of  $\lambda$  if there are no boxes below or to the right of it. Given a cell  $u = (i, j) \in [\lambda]$ , the *hook length* of  $u$ ,  $h(u) = \lambda_i - i + \lambda'_j - j + 1$ , is the number of cells to the right of  $u$  in row  $i$  and below  $u$  in column  $j$  including itself.

**Example 2.1.2.** There are 7 ways to partition 5; namely 5, 4+1, 3+2, 3+1+1, 2+2+1, 2+1+1+1, and 1+1+1+1+1. Below are the Young diagrams for each of the partitions. Observe that the first and seventh diagrams, second and sixth diagrams, and third and fifth diagrams are conjugates.

The fourth diagram is conjugate to itself.

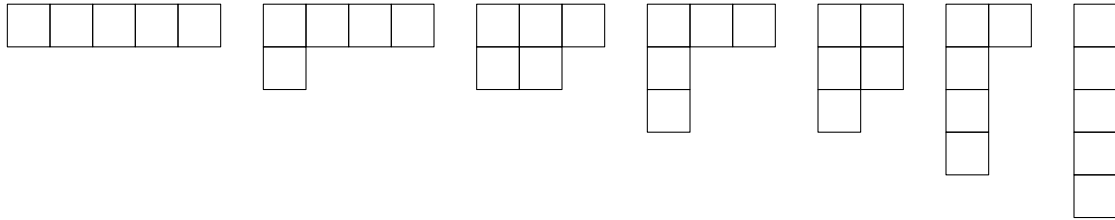


Figure 2.1. Young diagrams of the partitions of 5.

**Example 2.1.3.** Let  $\lambda = (5, 3, 3, 2, 1)$  and  $\mu = (3, 1, 1)$ . The cells in the diagram below that are unshaded form the skew Young diagram  $[\lambda/\mu]$ . Notice that  $|\lambda| = 14$ ,  $|\mu| = 5$ , and  $|\lambda/\mu| = 9$ . The inside corners are outlined in purple and the outside boxes are shown in green.

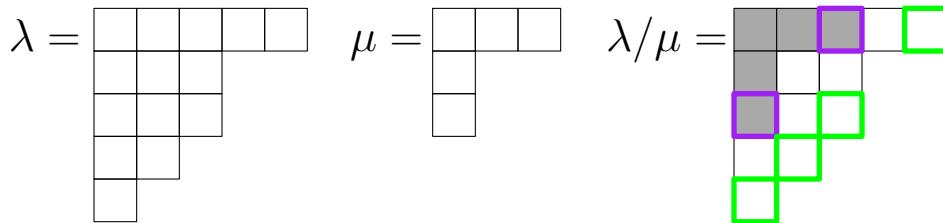


Figure 2.2. The skew diagram constructed from  $\lambda$  and  $\mu$ .

**Example 2.1.4.** For  $\lambda = (5, 3, 3, 2, 1)$ , below we show  $[\lambda]$  filled with the hook length of each cell. Notice that the Durfee square,  $\square^\lambda$ , is the  $(3, 3, 3)$  subdiagram outlined in red.

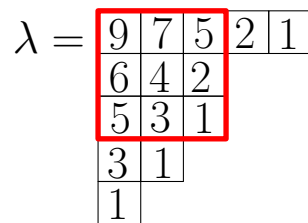


Figure 2.3. Hook lengths of a Young diagram.

The following are two of the many ways that we can fill Young diagrams:

**Definition 2.1.5.** Let  $\lambda$  be a partition of  $n$ . A *standard Young tableau* (SYT) is a filling of  $[\lambda]$  such that the numbers  $1, \dots, n$  are each used exactly once and the entries in the rows and columns are strictly increasing. We denote the set of all SYT of shape  $\lambda$  as  $SYT(\lambda)$ . The number of standard Young tableaux of shape  $\lambda$  is denoted by  $f^\lambda$ . Similarly, the set of all SYT of skew shape  $\lambda/\mu$  is written as  $SYT(\lambda/\mu)$  and the cardinality of this set is  $f^{\lambda/\mu}$ .

**Example 2.1.6.** Below are two SYT of shape  $\lambda = (5, 3, 3, 2, 1)$ .

$$T_1 = \begin{array}{|c|c|c|c|c|} \hline 1 & 2 & 3 & 4 & 5 \\ \hline 6 & 7 & 8 & & \\ \hline 9 & 10 & 11 & & \\ \hline 12 & 13 & & & \\ \hline 14 & & & & \\ \hline \end{array} \quad T_2 = \begin{array}{|c|c|c|c|c|} \hline 1 & 4 & 7 & 9 & 13 \\ \hline 2 & 5 & 12 & & \\ \hline 3 & 10 & 14 & & \\ \hline 6 & 11 & & & \\ \hline 8 & & & & \\ \hline \end{array}$$

Figure 2.4. Two elements of  $SYT(5,3,3,2,1)$ .

**Example 2.1.7.** Below are two examples of SYT of shape  $(5, 3, 3, 2, 1)/(3, 1, 1)$ .

$$T_1 = \begin{array}{|c|c|c|c|c|} \hline & & & 1 & 2 \\ \hline & 3 & 4 & & \\ \hline & 5 & 6 & & \\ \hline 7 & 8 & & & \\ \hline 9 & & & & \\ \hline \end{array} \quad T_2 = \begin{array}{|c|c|c|c|c|} \hline & & & 3 & 7 \\ \hline & 1 & 5 & & \\ \hline & 4 & 9 & & \\ \hline 2 & 8 & & & \\ \hline 6 & & & & \\ \hline \end{array}$$

Figure 2.5. Two standard Young tableaux of skew shape.

**Definition 2.1.8.** A *semistandard Young tableau* (SSYT) is a filling of  $[\lambda]$  such that the entries in the rows are increasing and the entries in the columns are strictly increasing. Notice that there is no restriction on how many times a value is used and there is no restriction on the maximum value of entries (unless otherwise noted). We denote the set of all SSYT of shape  $\lambda$  as  $SSYT(\lambda)$ . Similarly, the set of all SSYT of skew shape  $\lambda/\mu$  is written as  $SSYT(\lambda/\mu)$ .

**Example 2.1.9.** Shown below are two SSYT of shape  $\lambda = (5, 3, 3, 2, 1)$ .

$$T_1 = \begin{array}{|c|c|c|c|c|} \hline 1 & 1 & 1 & 1 & 1 \\ \hline 2 & 2 & 2 & & \\ \hline 3 & 3 & 3 & & \\ \hline 4 & 4 & & & \\ \hline 5 & & & & \\ \hline \end{array} \quad T_2 = \begin{array}{|c|c|c|c|c|} \hline 2 & 2 & 4 & 8 & 23 \\ \hline 3 & 7 & 15 & & \\ \hline 8 & 11 & 21 & & \\ \hline 9 & 19 & & & \\ \hline 16 & & & & \\ \hline \end{array}$$

Figure 2.6. Two elements of  $\text{SSYT}(5,3,3,2,1)$ .

**Remark 2.1.10.** In this paper,  $T$  will be used to represent a SYT or SSYT.

To keep track of what numbers are filling a SYT or SSYT, we define the content of a tableau.

**Definition 2.1.11.** Let  $\lambda$  be a partition and let  $T$  be a tableau of shape  $\lambda$ . We say the *content* of  $T$  is  $t = (t_1, t_2, \dots, t_m)$ , where  $t_i$  is the number of  $i$ 's in  $T$ . For any  $T \in \text{SYT}(\lambda)$ ,  $t = (1, 1, \dots, 1)$ . We say that  $|T| = \sum_i t_i i$ , that is,  $|T|$  is the sum of the entries of  $T$ .

**Example 2.1.12.** The SSYT from Figure 2.6 have contents  $t_1 = (5, 3, 3, 2, 1)$  and  $t_2 = (0, 2, 1, 1, 0, 0, 1, 2, 1, 0, 1, 0, 0, 0, 1, 1, 0, 0, 1, 0, 1, 0, 1)$ , respectively. So,  $|T_1| = 5+6+9+8+5 = 33$  and  $|T_2| = 4 + 3 + 4 + 7 + 16 + 9 + 11 + 15 + 16 + 19 + 21 + 23 = 148$ .

We can connect the set of semistandard Young tableaux to reverse plane partitions.

**Definition 2.1.13.** A *plane partition*  $\pi$  of shape  $\lambda$  is constructed by filling  $[\lambda]$  with non-negative integers where the entries are decreasing along rows and columns. The collection of all the plane partitions of shape  $\lambda$  is denoted  $\text{PP}(\lambda)$ , and the collection plane partitions of skew shape  $\lambda/\mu$  is denoted  $\text{PP}(\lambda/\mu)$ . A *reverse plane partition*  $\pi$  of shape  $\lambda$  is constructed by filling an array with non-negative integers where the entries are increasing along rows and columns. We denote the set of all reverse plane partitions of shape  $\lambda$  by  $\text{RPP}(\lambda)$ , and the set of all reverse plane partitions of skew shape by  $\text{RPP}(\lambda/\mu)$ . We say that  $\pi \in \text{RPP}(\lambda/\mu)$  has *support* of shape  $\rho/\nu$  if the cells that have non-zero entries form the shape  $\rho/\nu$ .

**Example 2.1.14.** Let  $\lambda = (3, 3, 1)$ . The following are two elements of  $\text{PP}(\lambda)$ .

$$\pi_1 = \begin{array}{|c|c|c|} \hline 0 & 0 & 0 \\ \hline 0 & 0 & 0 \\ \hline 0 & & \\ \hline \end{array} \quad \pi_2 = \begin{array}{|c|c|c|} \hline 5 & 3 & 1 \\ \hline 2 & 1 & 0 \\ \hline 2 & & \\ \hline \end{array}$$

Figure 2.7. Two plane partitions of shape  $(3,3,1)$ .

**Example 2.1.15.** Let  $\lambda = (3, 3, 1)$ . The following are two elements of  $\text{RPP}(\lambda)$ .

$$\pi_1 = \begin{array}{|c|c|c|} \hline 0 & 0 & 0 \\ \hline 0 & 0 & 0 \\ \hline 0 & & \\ \hline \end{array} \quad \pi_2 = \begin{array}{|c|c|c|} \hline 0 & 1 & 2 \\ \hline 3 & 3 & 4 \\ \hline 3 & & \\ \hline \end{array}$$

Figure 2.8. Two reverse plane partitions of shape  $(3,3,1)$ .

Notice that if we restrict  $\text{RPP}(\lambda/\mu)$  to have strictly increasing columns, we get  $\text{SSYT}(\lambda/\mu)$ . Therefore  $\text{SSYT}(\lambda/\mu) \subset \text{RPP}(\lambda/\mu)$ .

Two of the common combinatorial statistics that are related to SYT are descents and major index.

**Definition 2.1.16.** A *descent* of a SYT  $T$  is an index  $i$  such that  $i + 1$  appears in a row below  $i$ . The collection of descents of  $T$  is written as  $\text{Des}(T)$ . The *major index*, denoted  $\text{tmaj}(T)$ , is

$$\sum_{i \in \text{Des}(T)} i.$$

**Example 2.1.17.** Recall the second SYT in Figure 2.4.  $\text{Des}(T) = \{1, 2, 4, 5, 7, 9, 10, 13\}$  so  $\text{tmaj}(T) = 1 + 2 + 4 + 5 + 7 + 9 + 10 + 13 = 51$ .

When using  $\text{tmaj}(T)$ , we frequently also use a  $q$ -analogue of it.

**Definition 2.1.18.** For a variable  $q$  and positive integer  $i$ , the  $q$ -integer is defined as  $[i]_q = (1 + q + q^2 + \cdots + q^{i-1})$ . The  $q$ -factorial is defined by the following:  $[i]_q! = [i]_q [i-1]_q \cdots [2]_q [1]_q$ . We say a  $q$ -analogue of an algebraic expression is a new expression dependent on  $q$ , such that when the limit as  $q \rightarrow 1$  is applied, the result equals the original expression. For example,  $[n]_q!$  is a  $q$ -analogue of  $n!$ .

We can also define the major index of a permutation. Permutations are one of the most widely used objects in enumerative combinatorics.

**Definition 2.1.19.** Given the set  $S = \{1, \dots, n\}$ , we define a *permutation on  $S$* , denoted  $\sigma(S)$  as a bijective map from  $S$  to  $S$  such that  $\sigma$  reorders  $S$ . We consider permutations as words  $\omega = w_1 w_2 \dots w_n$  where  $w_i \in S$  and  $w_i = w_j$  if and only if  $i = j$ . The collection of all permutations on  $n$  elements is called the *symmetric group* and is denoted  $S_n$ . For  $\omega \in S_n$ , the *descent set* is given by  $\text{Des}(\omega) = \{i \mid w_i > w_{i+1}, 1 \leq i \leq n-1\}$ , and the *descent number* is  $\text{des}(\omega) = |\text{Des}(\omega)|$ . In a similar fashion, we have the *inversion number* of a permutation  $\omega$ , where  $\text{inv}(\omega) = |\{(i, j) \mid w_i > w_j, i < j\}|$ . The *sign of  $\omega$*  is defined as  $\text{sgn}(\omega) = (-1)^{\text{inv}(\omega)}$ . We call a permutation *odd* if  $\text{sgn}(\omega) = -1$ , and *even* otherwise. If permutation  $\omega$  has the form  $w_1 > w_2 < w_3 > w_4 < \dots$ , we say  $\omega$  is an *alternating permutation*. The number of alternating permutations of  $S_n$  is called the *Euler number*, denoted  $E_n$ .

**Example 2.1.20.** Let  $S = \{1, 2, 3\}$ . Then the set of all permutations on  $S$  is:

$S_3 = \{123, 132, 213, 231, 312, 321\}$ . The alternating permutations of  $S_3$  are 213 and 312. So  $E_3 = 2$ .

Let  $\omega = 43152 \in S_5$ . Then  $\text{Des}(\omega) = \{1, 2, 4\}$ , so  $\text{des}(\omega) = 3$  and  $\text{maj}(\omega) = 1 + 2 + 4 = 7$ . Also,  $\text{inv}(\omega) = |\{(1, 2), (1, 3), (1, 5), (2, 3), (2, 5), (4, 5)\}| = 6$ . Thus,  $\text{sgn}(\omega) = (-1)^6 = 1$ .

We can create monomials and symmetric polynomials based on the fillings of tableaux.

**Definition 2.1.21.** We say that a polynomial  $P(X_1, \dots, X_n)$  of  $n$  variables is *symmetric* if for  $\sigma \in S_n$ ,  $P(X_1, \dots, X_n) = P(X_{\sigma(1)}, \dots, X_{\sigma(n)})$ . Let  $T$  be a SSYT and  $t$  be the content of  $T$ . Let  $x^T$  be the *monomial for content  $t$*  of partition  $\lambda$ , defined as  $\prod_{i=1}^m (x_i)^{t_i}$ . The symmetric polynomial of shape  $\lambda$  with content  $t$  of variables  $\underline{x} = (x_1, \dots, x_m)$  is called the *Schur polynomial*, and is defined by  $s_\lambda(\underline{x}) = \sum_{T \in \text{SSYT}(\lambda)} \underline{x}^T$ . A  $q$ -analogue of the Schur polynomial is  $s_\lambda(1, q, \dots, q^m) = \sum_{T \in \text{SSYT}(\lambda)} q^{|\text{inv}(T)|}$ . A *complete homogeneous symmetric polynomial of degree  $k$*  is defined as  $h_k = \sum_{1 \leq i_1 \leq \dots \leq i_k \leq n} X_{i_1} \cdots X_{i_k}$ .

**Example 2.1.22.** Recall Figure 2.6. The contribution of the first tableau to  $s_{(5,3,3,2,1)}$  is  $x_1^5 x_2^3 x_3^3 x_4^2 x_5$ . The second tableau has contribution  $x_2^2 x_3 x_4 x_7 x_8^2 x_9 x_{11} x_{15} x_{16} x_{19} x_{21} x_{23}$  to  $s_{(5,3,3,2,1)}$ .

### 3. THE HOOK LENGTH FORMULA

The question of “How many?” is the fundamental question for the theory of enumerative combinatorics. Hence, it is natural to ask “How many standard Young tableaux of shape  $\lambda$  are there?” Further, we ask “How many semistandard Young tableaux with entries at most  $m$  of shape  $\lambda$  are there?” To answer these questions, mathematicians developed the hook length formula for SYT and the hook content formula for SSYT.

#### 3.1. History

In 1954, Frame, Robinson, and Thrall discovered the *hook length formula* (HLF).

**Theorem 3.1.1** ([3], Theorem 1). *Let  $\lambda$  be a partition of  $n$ . Then*

$$f^\lambda = \frac{n!}{\prod_{u \in [\lambda]} h(u)},$$

where  $h(u)$  is the hook length of the cell  $u$ .

**Example 3.1.2.** The number of SYT of shape  $\lambda = (5, 3, 3, 2, 1)$  is as follows.

$$f^{(5,3,3,2,1)} = \frac{14!}{9 \cdot 7 \cdot 5 \cdot 2 \cdot 1 \cdot 6 \cdot 4 \cdot 2 \cdot 5 \cdot 3 \cdot 1 \cdot 3 \cdot 1 \cdot 1} = 14 \cdot 13 \cdot 11 \cdot 8 \cdot 4 = 64064$$

Frame, Robinson, and Thrall’s proof relies on the Frobenius formula [18], which computes the characters of the irreducible representations of  $S_n$  corresponding to a partition  $\lambda$ . Although their formula has been widely used, their proof of the HLF has not. Many feel that the proof is unintuitive. A proof that more clearly incorporates the role of the hook lengths was developed by Hillman and Grassl [5].

Their strategy begins with finding a generating function based on the number of  $\pi \in \text{RPP}(\lambda)$ . Next, they define a bijection between the set  $\text{RPP}(\lambda)$  and the set of  $s$ -tuples of the multiplicities of hook lengths. They use this bijection to prove that the generating function for  $\text{RPP}(\lambda)$  is the same the generating function for the set of  $s$ -tuples, thus, proving the HLF.



### 3.2. Hook Content Formula

The enumeration formula for SSYT is called the *hook content formula*. This counts the number of SSYT of shape  $\lambda$  with entries at most  $m$ . The hook content formula was alluded to by Littlewood and Richardson, but the first precise statement was given by Stanley [21].

Now let us state the hook content formula (HCF) for SSYT of shape  $\lambda$  with entries at most  $m$ .

**Theorem 3.2.1** ([2, 21]). *The number of SSYT of shape  $\lambda$  and entries at most  $m$  is computed by*

$$\prod_{u \in [\lambda]} \frac{m + c(u)}{h(u)},$$

where  $c(u) = j - i$  for cell  $u = (i, j)$ .

**Remark 3.2.2.** *We call  $c(u)$  the content of cell  $u$  for  $u \in [\lambda]$ .*

**Example 3.2.3.** Recall Figure 2.6. Let us compute the number of SSYT(5, 3, 3, 2, 1) with entries at most 6. The number of SSYT of shape (5,3,3,2,1) with entries at most  $m = 6$  equals  $\frac{6 \cdot 7 \cdot 8 \cdot 9 \cdot 10 \cdot 5 \cdot 6 \cdot 7 \cdot 4 \cdot 5 \cdot 6 \cdot 3 \cdot 4 \cdot 2}{9 \cdot 7 \cdot 5 \cdot 2 \cdot 1 \cdot 6 \cdot 4 \cdot 2 \cdot 5 \cdot 3 \cdot 1 \cdot 2 \cdot 1 \cdot 1} = 20160$ .

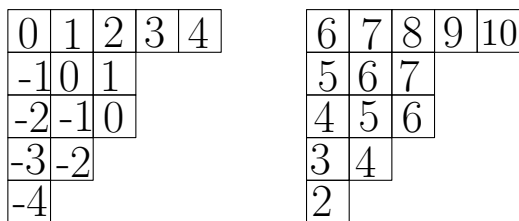


Figure 3.1. The first Young diagram above shows the content of each cell. The second Young diagram shows the values of  $m + c(u)$  for each cell.

### 3.3. $q$ -analogues of the Hook Length Formula and Hook Content Formula

There are numerous other versions and generalizations of the HLF and HCF. One generalization, due to Stanley, is a  $q$ -analogue of the HCF.

**Theorem 3.3.1** ([21], Theorem 7.21.2). *Let  $\lambda$  be a partition. Then the Schur polynomial  $s_\lambda(x_1, \dots, x_m)$*

with  $x_i = q^{i-1}$  is given by

$$s_\lambda(1, q, \dots, q^{m-1}) = q^{b(\lambda)} \prod_{u \in [\lambda]} \frac{[m + c(u)]_q}{[h(u)]_q}$$

with  $b(\lambda) = \sum_i (i-1)\lambda_i$ .

Theorem 3.3.1 has the following corollaries.

**Corollary 3.3.2** ([21], Corollary 7.21.3). *For any partition  $\lambda$ , we have*

$$s_\lambda(1, q, q^2, \dots) = q^{b(\lambda)} \prod_{u \in \lambda} \frac{1}{1 - q^{h(u)}},$$

where  $b(\lambda) = \sum_i (i-1)\lambda_i$ .

**Remark 3.3.3.** *One can derive the HLF from its  $q$ -analogue by Stanley's theory of  $P$ -partitions [20] or by a geometric argument of Pak [16]. Pak's argument is centered around taking the volume of cones of functions.*

By taking the limit as  $q$  approaches 1 in Corollary 3.3.2, the HLF is obtained. Therefore, Corollary 3.3.2 is considered a combinatorial  $q$ -analogue of the HLF.

**Corollary 3.3.4** ([21], Corollary 7.21.5). *Let  $\lambda$  be a partition of  $n$ . Then,*

$$\sum_{T \in SYT(\lambda)} q^{\text{maj}(T)} = \frac{q^{b(\lambda)} [n]_q!}{\prod_{u \in [\lambda]} [h(u)]_q}.$$

## 4. HOOK LENGTH FORMULA FOR SKEW SHAPES

Naturally, in mathematics, when a new object is defined that is derived from another, we try to see what results from the known object can be adapted for the new. Since we know the hook length formula, it is natural to try and find a formula that enumerates skew standard tableaux of shape  $\lambda/\mu$ . In this chapter, we will discuss this recently found formula and its proofs.

### 4.1. Naruse Hook Length Formula

In 2014, Naruse found the following formula and presented it, unproven, at a conference:

**Theorem 4.1.1** (Naruse Hook Length Formula (NHLF), [14]). *Let  $\lambda, \mu$  be partitions such that  $\mu \subset \lambda$ . Then*

$$f^{\lambda/\mu} = |\lambda/\mu|! \sum_{D \in \varepsilon(\lambda/\mu)} \prod_{u \in [\lambda] \setminus D} \frac{1}{h(u)}.$$

Subsequently, the formula was proven by Morales, Pak, and Panova in three different ways [10]. We will discuss these different proofs of the NHLF. Before we can see an example of the NHLF, we must first introduce excited diagrams.

**Definition 4.1.2** ([14]). Let  $\lambda/\mu$  be a skew partition and  $D$  be a subset of the Young diagram of  $\lambda$ . A cell  $u = (i, j) \in D$  is called *active* if  $(i+1, j)$ ,  $(i, j+1)$  and  $(i+1, j+1)$  are all in  $[\lambda] \setminus D$ . For an active cell  $u \in D$ ,  $\alpha_{u(D)}$  is the set obtained by replacing  $(i, j)$  in  $D$  by  $(i+1, j+1)$ . This process is called an *excited move*. An *excited diagram* of  $\lambda/\mu$  is a sub-diagram of  $\lambda$  obtained from the Young diagram of  $\mu$  after a sequence of excited moves on excited cells. Let  $\varepsilon(\lambda/\mu)$  be the set of excited diagrams of  $\lambda/\mu$  and  $e(\lambda/\mu) = |\varepsilon(\lambda/\mu)|$ .

**Remark 4.1.3.** *Notice that if  $\mu = \emptyset$ , then there is a unique excited diagram  $D = \emptyset$ . In this case, the NHLF simplifies to the HLF.*

**Example 4.1.4.** Let  $\lambda = (5, 3, 3, 2, 1)$  and  $\mu = (3, 1, 1)$ . The shape  $\lambda/\mu$  is an excited diagram with  $D = [\mu]$  and no excited moves completed. In Figure 4.1, the cell outlined in red is active since the cells below, right, and diagonal from it are in  $[\lambda/\mu]$ . We complete an excited move to get another excited diagram. There are no other spaces we can move that cell in  $D$ , so we move to the next

cell, outlined in blue. This is another active cell. We do another excited move to get our last excited diagram. This is the final excited diagram, since there are no other cells in  $D$  that have the surrounding three cells in  $\lambda/\mu$ .

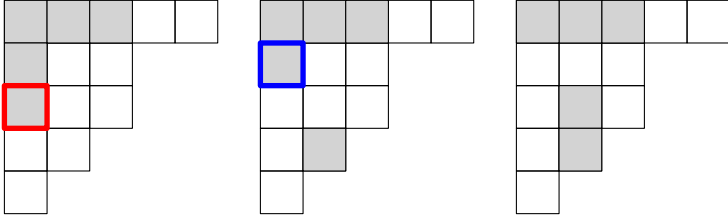


Figure 4.1. The excited diagrams of shape  $(5, 3, 3, 2, 1)/(3, 1, 1)$ .

Now let us use the NHLF to find the number of SYT of shape  $\lambda/\mu$ .

**Example 4.1.5.** For  $\lambda$  and  $\mu$  as in the previous example, we observe that  $|\lambda/\mu| = 9$ . In figure 4.2, we have the three excited diagrams of shape  $(5, 3, 3, 2, 1)/(3, 1, 1)$  filled with their hook lengths. Then, by the NHLF,

$$f^{\lambda/\mu} = 9! \left( \frac{1}{2 \cdot 1 \cdot 4 \cdot 2 \cdot 3 \cdot 1 \cdot 3 \cdot 1 \cdot 1} + \frac{1}{2 \cdot 1 \cdot 4 \cdot 2 \cdot 5 \cdot 3 \cdot 1 \cdot 3 \cdot 1} + \frac{1}{2 \cdot 1 \cdot 6 \cdot 4 \cdot 2 \cdot 5 \cdot 1 \cdot 3 \cdot 1} \right) = 3276.$$

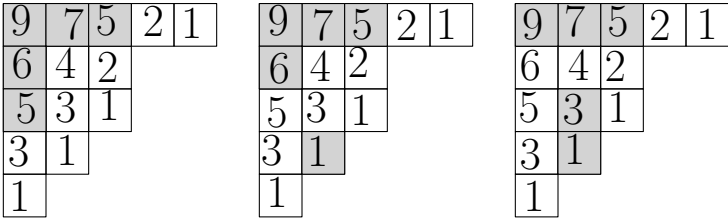


Figure 4.2. Hook lengths in the excited diagrams of shape  $(5, 3, 3, 2, 1)/(3, 1, 1)$ .

#### 4.2. Proof of the NHLF Using Excited Diagrams

Similar to the HLF having a  $q$ -analogue, there is also a  $q$ -analogue from which the NHLF can be derived.

**Theorem 4.2.1** ([10], Theorem 1.4). *For  $\lambda/\mu$ , we have*

$$s_{\lambda/\mu}(1, q, q^2, \dots) = \sum_{S \in \varepsilon(\lambda/\mu)} \prod_{(i,j) \in [\lambda] \setminus S} \frac{q^{\lambda'_j - i}}{1 - q^{h(i,j)}}.$$

In Stanley's theory of  $(P, \omega)$ -partitions [20], he shows the following equality:

$$s_{\lambda/\mu}(1, q, q^2, \dots) = \frac{\sum_T q^{\text{tmaj}(T)}}{(1-q)(1-q^2) \cdots (1-q^n)} \quad (4.1)$$

where  $T \in \text{SYT}(\lambda/\mu)$ . Now we will outline the proof found in [10] that the  $q$ -analogue of the NHLF implies the NHLF.

*Proof of Theorem 4.1.1.* We begin by multiplying both sides of the equation (4.1) by  $(1-q)(1-q^2) \cdots (1-q^n)$ . Using Theorem 4.2.1, we have

$$\sum_{T \in \text{SYT}(\lambda/\mu)} q^{\text{tmaj}(T)} = \prod_{i=1}^n (1-q^i) \sum_{D \in \varepsilon(\lambda/\mu)} \prod_{(i,j) \in [\lambda] \setminus D} \frac{q^{\lambda'_i - i}}{1 - q^{h(i,j)}}.$$

Since all of the excited diagrams  $D \in \varepsilon(\lambda/\mu)$  have the same size,  $|\lambda/\mu|$ , we obtain the NHLF by taking the limit as  $q$  approaches 1. □

### 4.3. Proof of the NHLF Using Pleasant Diagrams

The second proof of the NHLF by Morales, Pak, and Panova [10] relies on the relationship between pleasant diagrams and excited diagrams.

**Definition 4.3.1** ([5]). We define the *Hillman-Grassl map*,  $\Phi$ , by using the following process. Let  $\pi \in \text{RPP}(\lambda)$  and let  $\mathcal{A}$  be an array of zeros of shape  $\lambda$ . The following defines the map  $\Phi$ . Let  $\mathbf{p}$  be a path of north steps,  $(0, 1)$ , and east steps,  $(1, 0)$ , in  $\pi$  such that:

1. The path  $\mathbf{p}$  starts at the most southwest nonzero entry in  $\pi$ . Denote  $c_s$  by the column of the starting entry.
2. If  $\mathbf{p}$  reaches  $(i, j)$  and  $\pi_{i,j} = \pi_{i-1,j} > 0$ , then  $\mathbf{p}$  will move north to cell  $(i-1, j)$ . However, if  $0 < \pi_{i,j} < \pi_{i-1,j}$ , then  $\mathbf{p}$  will move east to cell  $(i, j+1)$ .

3. When there are no possible east moves remaining,  $\mathbf{p}$  terminates. Denote  $r_f$  to be the row of the final entry.

Now let  $\pi'$  be constructed by subtracting 1 from every entry in the path  $\mathbf{p}$ . Notice that  $\pi' \in \text{RPP}(\lambda)$ . Then in  $\mathcal{A}$ , add 1 to position  $A_{c_s, r_f}$  to obtain  $A'$ . Continue the process until the reverse plane partition has only zeros for entries.

**Theorem 4.3.2** ([5]). *Let  $\mathcal{A}(\lambda)$  denote the set of all fillings of  $[\lambda]$  with nonnegative integers. The Hillman-Grassl map  $\Phi : \text{RPP}(\lambda) \rightarrow \mathcal{A}(\lambda)$  is a bijection.*

We next discuss the application of the Hillman-Grassl map to pleasant diagrams, which establishes a theorem required in the proof of Theorem 4.1.1.

**Definition 4.3.3** ([10, 11]). Let  $\lambda$  be a partition. For an integer  $k$ , where  $1 - \ell(\lambda) \leq k \leq \lambda_1 - 1$ , let  $\mathbf{d}_k$  be the diagonal  $\{(i, j) \in \lambda/\mu \mid i - j = k\}$ . Let  $\square_k^\lambda$  be the largest rectangle with  $i$  rows and  $i + k$  columns that is a subdiagram of  $\lambda$  starting at  $(1, 1)$ . We say that a diagram  $S \subset [\lambda]$  is a *pleasant diagram* of  $\lambda/\mu$  if, for all  $k \in \mathbb{Z}$ , with  $1 - \ell(\lambda) \leq k \leq \lambda_1 - 1$ , the subarray  $S_k := S \cap \square_k^\lambda$  has no descending chain larger than the length  $s_k$  of the diagonal  $\mathbf{d}_k$  of  $\lambda/\mu$ . Let  $\mathcal{P}(\lambda/\mu)$  be the set of pleasant diagrams of  $\lambda/\mu$ . Let  $p(\lambda/\mu) = |\mathcal{P}(\lambda/\mu)|$ .

**Example 4.3.4** ([11]). Let  $\lambda = (2, 2)$  and  $\mu = (1)$ . The pleasant diagrams cannot have descending chains in  $S_{-1}$ ,  $S_0$ , and  $S_1$  of sizes greater than one. Hence, we must exclude the subsets of  $[\lambda] = \{(1, 1), (1, 2), (2, 1), (2, 2)\}$  that contain the descending chain  $((1, 1), (2, 2))$ . So of the sixteen subsets of  $[\lambda]$ , twelve are pleasant diagrams. Below are all of the subsets of  $[\lambda]$ , with the pleasant diagrams outlined in blue.

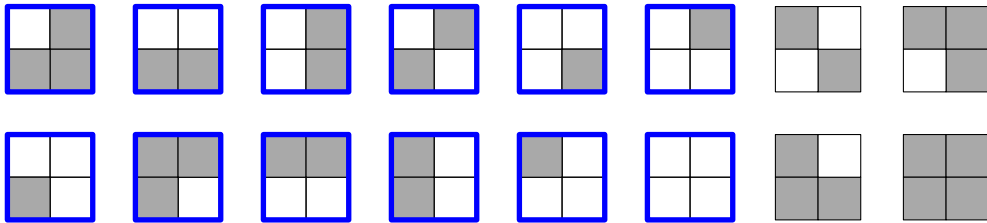


Figure 4.3. The pleasant diagrams of shape  $(2,2)$ .

The second proof of the NHLF also requires two theorems from [10], which we give without proof.

**Theorem 4.3.5** ([10], Theorem 6.3). *A reverse plane partition  $\pi \in RPP(\lambda)$  has support in a skew shape  $\lambda/\mu$  if and only if the support of  $\Phi(\pi)$  is a pleasant diagram in  $\mathcal{P}(\lambda/\mu)$ . Moreover,*

$$\sum_{\pi \in RPP(\lambda/\mu)} q^{|\pi|} = \sum_{S \in \mathcal{P}(\lambda/\mu)} \left[ \prod_{u \in S} \frac{q^{h(u)}}{1 - q^{h(u)}} \right].$$

**Theorem 4.3.6** ([10], Theorem 6.5). *A pleasant diagram  $S \in \mathcal{P}(\lambda/\mu)$  has size  $|S| \leq |\lambda/\mu|$ .  $S$  has maximal size  $|S| = |\lambda/\mu|$  if and only if the complement  $[\lambda] \setminus S = \bar{S}$  is an excited diagram in  $\varepsilon(\lambda/\mu)$ .*

The proof also requires a theorem given by Stanley in [20]. Before we can give the statement of the proof, we need to establish some definitions and notation. The following two sets of definitions can be found in [20].

**Definition 4.3.7** ([20], Section 3.1). A *partially ordered set*  $P$  (*poset*) is a set with an associated binary relation, which we denote  $\leq$ , such that

- for all  $x \in P$ ,  $x \leq x$ ,
- if  $x \leq y$  and  $y \leq x$ , then  $x = y$ , and
- if  $x \leq y$  and  $y \leq z$ , then  $x \leq z$ .

These properties are called *reflexivity*, *antisymmetry*, and *transitivity*, respectively.

**Remark 4.3.8.** *We can view Young diagrams as posets by considering the following: For two cells of  $[\lambda/\mu]$ ,  $u = (i, j)$  and  $v = (i', j')$ , we say  $u \leq v$  in the poset  $P_{\lambda/\mu}$  if and only if  $i \leq i'$  and  $j \leq j'$ .*

**Definition 4.3.9** ([20], Section 3.15). Let  $P$  be a finite poset with  $p$  elements. Then a bijection  $\omega: P \rightarrow \{1, \dots, p\}$  is called a *labeling* of  $P$ . We define a  $(P, \omega)$ -*partition* as a map  $\sigma: P \rightarrow \mathbb{N}$  that satisfies:

- if  $x \leq y$  in  $P$ , then  $\sigma(x) \geq \sigma(y)$  ( $\sigma$  is called *order-reversing*).
- if  $x < y$  and  $\omega(x) > \omega(y)$ , then  $\sigma(x) > \sigma(y)$ .

If  $\sum_{t \in P} \sigma(t) = n$ , then  $\sigma$  is a  $(P, \omega)$ -partition of  $n$ . The fundamental generating function associated with  $(P, \omega)$ -partitions is given by

$$F_{P, \omega}(x_1, \dots, x_p) = \sum_{\sigma} x_1^{\sigma(t_1)} \cdots x_p^{\sigma(t_p)},$$

where the sum is over all  $\sigma \in (P, \omega)$ -partitions. A *linear extension* of a poset is a labeling  $\omega$  such that  $\omega(x) < \omega(y)$  implies  $x < y$ . We denote the set of all linear extensions of  $P$  by  $\omega$  as  $\mathcal{L}(P)$ . Let  $a(n)$  be the number of  $(P, \omega)$ -partitions of  $n$ . Define the generating function  $G_{P, \omega}(x) = \sum_{n \geq 0} a(n)x^n$ .

Also, let  $W_{P, \omega}(x) = \sum_{\omega \in \mathcal{L}(P)} x^{\text{maj}(\omega)}$ .

**Theorem 4.3.10** ([20], Theorem 3.15.7). *We have*

$$G_{P, \omega}(x) = \frac{W_{P, \omega}(x)}{(1-x)(1-x^2) \cdots (1-x^p)}.$$

This theorem of Stanley's is used to begin the second proof of the NHLF from [10].

*Proof of Theorem 4.1.1.* Let  $n = |\lambda/\mu|$  and consider the poset  $P_{\lambda/\mu}$  of the skew diagram  $\lambda/\mu$ . Then,

$$\sum_{\pi \in \text{RPP}(\lambda/\mu)} q^{|\pi|} = \frac{W_{P_{\lambda/\mu}, \omega}(q)}{\prod_{i=1}^n (1-q^i)}. \quad (4.2)$$

If we multiply both sides of equation (4.2) by  $\prod_{i=1}^n (1-q^i)$ , then we have

$$\left( \prod_{i=1}^n (1-q^i) \right) \sum_{S \in \mathcal{P}(\lambda/\mu)} \prod_{u \in S} \frac{q^{h(u)}}{1-q^{h(u)}} = \sum_{\omega \in \mathcal{L}(P_{\lambda/\mu})} q^{\text{maj}(\omega)}. \quad (4.3)$$

By Theorem 4.3.6, the pleasant diagrams  $S \in \mathcal{P}(\lambda/\mu)$  have size  $|S| \leq n$ , and  $|S| = n$  when  $\bar{S} \in \varepsilon(\lambda/\mu)$ . By letting  $q \rightarrow 1$  in (4.3),  $\sum_{\omega \in \mathcal{L}(P_{\lambda/\mu})} q^{\text{maj}(\omega)}$  becomes  $f^{\lambda/\mu}$ . Also, the left-hand side of the equation transforms to

$$\sum_{S \in \varepsilon(\lambda/\mu)} \prod_{u \in \bar{S}} \frac{1}{h(u)}.$$



That is, we have

$$f^{\lambda/\mu} = |\lambda/\mu|! \sum_{S \in \varepsilon(\lambda/\mu)} \prod_{u \in S} \frac{1}{h(u)}$$

as desired. □

#### 4.4. Proof of the NHLF Using Shadow Lines

The third proof of the NHLF provided in [10] is based on Stanley's theory of  $P$ -partitions and the enumeration of pleasant diagrams of shape  $\lambda/\mu$ . However, to use the enumeration, we require the following somewhat conceptual definitions.

**Definition 4.4.1** ([23]). Consider  $S \in \mathcal{P}(\lambda/\mu)$ . First, we visualize a light source located in the  $(1, 1)$  cell of  $[\lambda]$  and any elements of  $S$  cast shadows along the axes positioned on the north and west borders of  $[\lambda]$ . The boundary of the casted shadows forms the *shadow line*  $L_1$ . We can recursively define the set of  $L_i$ 's by the following method:

1. Delete any of the elements in  $S$  that were in the previous shadow lines.
2. Designate the shadow line formed by the remaining elements of  $S$  as the new shadow line.

Continue the above process until there are no remaining elements of  $S$ .

Now on excited diagrams, we discuss the idea of excited peaks.

**Definition 4.4.2** ([11]). Let  $D \in \varepsilon(\lambda/\mu)$ . We call the subset  $[\lambda] \setminus D$ , denoted  $\Lambda(D)$ , the set of *excited peaks*. For  $D$  with active cell  $u = (i, j)$ , the excited peaks of  $\alpha_u(D)$  are  $\lambda(\alpha_u(D)) = (\Lambda(D) \setminus \{(i, j+1), (i+1, j)\}) \cup \{u\}$ . When  $[\mu] \in \varepsilon(\lambda/\mu)$ , then  $\Lambda([\mu]) = \emptyset$ . We denote the number of excited peaks of  $D$  as  $\text{expk}(D) := |\Lambda(D)|$ .

Using the definition of excited peaks, the number of pleasant diagrams of skew shape can be enumerated.

**Theorem 4.4.3** ([11], Theorem 6.14). *Let  $\lambda$  and  $\mu$  be partitions with  $\mu \subset \lambda$ .*

$$|\mathcal{P}(\lambda/\mu)| = \sum_{D \in \varepsilon(\lambda/\mu)} 2^{|\lambda/\mu| - \text{expk}(D)}.$$

**Corollary 4.4.4** ([11], Corollary 6.17). *Let  $\lambda$  and  $\mu$  be partitions with  $\mu \subset \lambda$ .*

$$\sum_{\pi \in RPP(\lambda/\mu)} q^{|\pi|} = \sum_{D \in \varepsilon(\lambda/\mu)} q^{a'(D)} \prod_{u \in [\lambda] \setminus D} \frac{1}{1 - q^{h(u)}}$$

Now we can give the third proof of the NHLF from [10].

*Proof of Theorem 4.1.1.* We begin the proof by recalling the generating function from Theorem 4.3.10. Then we procure (4.2). When we multiply both sides of (4.2) by  $\prod_{i=1}^n (1 - q^i)$  for  $n = |\lambda/\mu|$  and use Corollary 4.4.4, we arrive at the following:

$$\sum_{\omega \in \mathcal{L}(\mathcal{P}_{\lambda/\mu})} q^{\text{maj}(\omega)} = \prod_{i=1}^n (1 - q^i) \sum_{D \in \varepsilon(\lambda/\mu)} q^{a'(D)} \prod_{u \in [\lambda] \setminus D} \frac{1}{1 - q^{h(u)}}.$$

Now we take the limit of the above equation as  $q \rightarrow 1$ . Therefore, the NHLF has been proved.  $\square$

## 5. FUN WITH EXCITED DIAGRAMS

Excited diagrams are not only crucial in the development of the NHLF, but have surprising results that are connected to Catalan objects. The *Catalan numbers* were named after Eugéne Charles Catalan. This is a sequence of numbers that arises in many counting problems.

### 5.1. Catalan Numbers and Objects

Any objects that are counted by the Catalan numbers are *Catalan objects*. The sequence of Catalan numbers is 1, 1, 2, 5, 14, 42, 132, . . . . The  $n$ -th Catalan number is found by using one of the following equivalent formulas:

$$C_n = \frac{1}{n+1} \binom{2n}{n} = \frac{(2n)!}{(n+1)!n!} = \binom{2n}{n} - \binom{2n}{n+1} = \prod_{k=2}^n \frac{n+k}{k}.$$

Two types of the Catalan objects that are relevant to this paper are  $SYT(\lambda)$  where  $\lambda = (n, n)$  and Dyck paths. See [19] for many more Catalan objects.

**Definition 5.1.1.** A *Dyck path* is a path in the plane that begins at  $(0, 0)$  and ends  $(2n, 0)$ , using only up-steps  $(1, 1)$  and down-steps  $(1, -1)$ , and never going below the  $x$ -axis.

**Proposition 5.1.2** ([19]). *The number of Dyck paths from  $(0, 0)$  to  $(2n, 0)$  equals the  $n$ -th Catalan number,  $C_n$ .*

*Proof.* Consider all paths from  $(0, 0)$  to  $(2n, 0)$  consisting of up-steps  $(1, 1)$  and down-steps  $(1, -1)$ . Each path has  $n$  up-steps and  $n$  down-steps. Thus, there are  $\binom{2n}{n}$  possible paths. However, some of these paths will go below the  $x$ -axis. That is, not all of the  $\binom{2n}{n}$  paths are Dyck paths. For any non-Dyck path, pick the point with the most negative  $y$ -coordinate. If there are multiple points with this same  $y$ -coordinate, then pick the point furthest to the left. Now change the down-step immediately to the left of this point to an up-step. But now the path will have  $n + 1$  up-steps and  $n - 1$  down-steps, resulting in an endpoint of  $(2n, 2)$ . Hence, we have constructed a map  $f: \{\text{non-Dyck paths from } (0, 0) \text{ to } (2n, 0)\} \rightarrow \{\text{all paths from } (0, 0) \text{ to } (2n, 2)\}$ .

Now we construct the inverse map,  $f^{-1}$ . For a path from  $(0, 0)$  to  $(2n, 2)$ , find the point

with the most negative  $y$ -coordinate. This time, if there are multiple points having the same most negative  $y$ -coordinate, pick the point furthest to the right. Change the up-step immediately to the right of this point to a down-step. This is the inverse of  $f$  since it will change the extra up-step created by  $f$  to a down-step, leaving the rest of the path unchanged. Thus,  $f$  is a bijection. Since the set of all paths from  $(0,0)$  to  $(2n,2)$  are counted by  $\binom{2n}{n+1}$ , the number of Dyck paths from  $(0,0)$  to  $(2n,0)$  is  $\binom{2n}{n} - \binom{2n}{n+1} = C_n$ .  $\square$

**Proposition 5.1.3** ([19]). For  $\lambda = (n, n)$ ,  $|SYT(\lambda)| = C_n$ .

*Proof.* We show this class of SYT are Catalan objects by constructing a bijection with Dyck paths. First, notice that  $|\lambda| = 2n$  and the length of a Dyck path is  $2n$ . Numbers in the top row of the SYT correspond to up-steps and numbers in the bottom row of the SYT correspond to down-steps. That is, for  $i$  in the top row, the  $i$ -th step of the corresponding Dyck path is an up-step, and for  $i$  in the bottom row, the  $i$ -th step is a down step. The condition that the rows and columns are increasing corresponds exactly to the condition that the Dyck path cannot go below the  $x$ -axis.  $\square$

**Example 5.1.4.** Below are the Catalan objects for Dyck paths of length  $2n$  and SYT of shape  $\lambda = (n, n)$ , for  $n = 1, 2, 3$ .

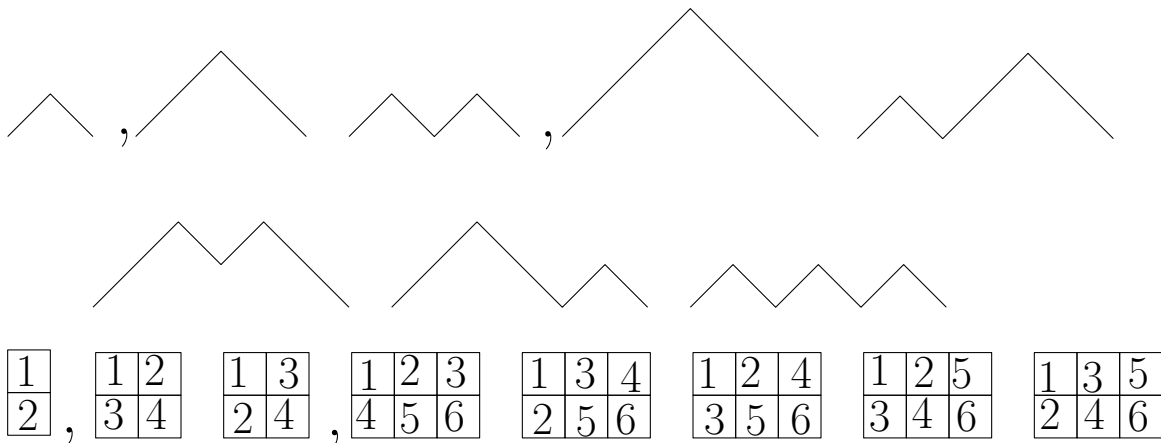


Figure 5.1. Catalan objects.

**Remark 5.1.5** ([9]). *The following is a notable determinant:*

$$\begin{bmatrix} C_1 & C_2 & \cdots & C_n \\ C_2 & C_3 & \cdots & C_{n+1} \\ \vdots & \vdots & \ddots & \vdots \\ C_n & C_{n+1} & \cdots & C_{2n} \end{bmatrix} = 1.$$

## 5.2. Catalan Numbers and Excited Diagrams

In this section, we discuss a corollary that shows the number of excited diagrams of staircase shape is enumerated by a determinant of Catalan numbers.

**Definition 5.2.1.** A Young diagram of shape  $\delta_n = (n-1, n-2, \dots, 2, 1)$  is *staircase shaped*. Further, the skew diagram  $\delta_{n+2k}/\delta_n$  is called *thick strip*.

**Corollary 5.2.2** ([11], Corollary 8.1). *The number of excited diagrams of thick strip shape is given by the following:  $e(\delta_{n+2}/\delta_n) = C_n$ ,  $e(\delta_{n+4}/\delta_n) = C_n C_{n+2} - C_{n+1}^2$ , and in general,*

$$e(\delta_{n+2k}/\delta_n) = \det[C_{n-2+i+j}]_{i,j=1}^k = \prod_{1 \leq i < j \leq n} \frac{2k+i+j-1}{i+j-1}. \quad (5.1)$$

To prove this interesting corollary, we will introduce another type of tableau.

**Definition 5.2.3** ([10]). Let  $\mu$  be a partition. Let  $\mathbf{f} = (\mathbf{f}_1, \mathbf{f}_2, \dots, \mathbf{f}_{\ell(\mu)})$  be a sequence of positive integers, which we call a *flag*. Given a flag  $\mathbf{f}$ , the *flagged tableaux* of shape  $\mu$  are a subset of  $SSYT(\mu)$  such that the entries in row  $i$  are at most  $f_i$ . We write the set of flagged tableaux of shape  $\mu$  and flag  $\mathbf{f}$  as  $\mathcal{F}(\mu, \mathbf{f})$ . A cell  $(x, y)$  of  $T$  in  $\mathcal{F}(\mu, \mathbf{f})$  is *active* if increasing  $T_{x,y}$  by 1 gives a flagged tableau,  $T'$ , in  $\mathcal{F}(\mu, \mathbf{f})$ . We call this map a *flagged move*, denoted  $\alpha'_{x,y}(T) = T'$ . We denote the tableau of shape  $\mu$  with all entries in row  $i$  equal to  $i$  as  $T_\mu$ .

The number of  $\mathcal{F}(\mu, \mathbf{f})$  is given by the following proposition:

**Proposition 5.2.4** ([4, 24]). *Using the above notation, we have the following equalities:*

$$|\mathcal{F}(\mu, \mathbf{f})| = \det [h_{\mu_i - i + j}(\mathbf{f}_i)]_{i,j=1}^{\ell(\mu)} = \det \left[ \begin{pmatrix} \mathbf{f}_i + \mu_i - i + j - 1 \\ \mu_i - i + j \end{pmatrix} \right]_{i,j=1}^{\ell(\mu)}$$

where  $h_k(x_1, x_2, \dots)$  is the complete homogeneous symmetric function.

**Definition 5.2.5** ([10]). We define the flag  $\mathbf{f}^{\lambda/\mu} = (\mathbf{f}_1, \mathbf{f}_2, \dots, \mathbf{f}_{\ell(\mu)})$  as follows. Let  $\mathbf{f}_i$  be the row of  $\lambda$  in which the last cell of row  $i$  of  $\mu$  ends after applying all possible excited moves to  $\mu$ . We define a map  $\phi: \varepsilon(\lambda/\mu) \rightarrow \mathcal{F}(\mu, \mathbf{f}^{\lambda/\mu})$  as follows. Let  $(i, j)$  be a box in the excited diagram  $D$ . Let  $(x_i, y_j)$  be the position of the box after applying excited moves to the excited diagram until no more are possible. Construct  $T := \phi(D)$  by putting  $j$  in the box  $(x_i, y_j)$  of  $\mu$ . That is,  $T_{x_i, y_j} := j$ . We do this for each box in the excited diagram.

**Proposition 5.2.6** ([10], Proposition 3.6). *The map  $\phi: \varepsilon(\lambda/\mu) \rightarrow \mathcal{F}(\mu, \mathbf{f}^{\lambda/\mu})$  is a bijection. Moreover,  $e(\lambda/\mu) = |\mathcal{F}(\mu, \mathbf{f}^{\lambda/\mu})|$ .*

*Proof.* [10] We begin by proving that  $\phi$  is well-defined. That is, we want to show that  $T = \phi(D)$  is a SSYT through induction on the number of excited moves of  $D$ . Assume  $D \in \varepsilon(\lambda/\mu)$ . Notice that  $\phi([\mu]) = T_\mu$ , which is a SSYT. Now,  $T = \phi(D)$  is a SSYT and that  $D' = \alpha_{(i,j)}(D)$  corresponds to  $(x_i, y_j) \in [\mu]$  for an active cell  $(i, j) \in D$ . We get  $T' = \phi(D)$  from  $T$  by adding 1 to the entry  $T_{x_i, y_j} = i$  and leaving the remaining entries unchanged. For  $(x_i + 1, y_j) \in [\mu]$ , since  $(i + 1, j)$  is not a cell in  $D$ , the cell of the diagram corresponding to  $(x_i + 1, y_j)$  is located in a row below  $i + 1$ . Hence  $T'_{x_i, y_j} = i + 1 < T_{x_i + 1, y_j} = T'_{x_i + 1, y_j}$ . Similarly, if  $(x_i, y_j + 1) \in [\mu]$ , since  $(i, j + 1)$  is not a cell in  $D$ , then the cell of the diagram corresponding to  $(x_i, y_j + 1)$  is located in a row below  $i$ . Thus,  $T'_{x_i, y_j} = i + 1 \leq T_{x_i, y_j + 1} = T'_{x_i, y_j + 1}$ . Therefore,  $T' \in \text{SSYT}(\lambda/\mu)$ .

Now, we want to show that  $T \in \mathcal{F}(\mu, \mathbf{f}^\lambda)$ . Let  $D \in \varepsilon(\lambda/\mu)$ . If the cell  $(i, j) \in D$  corresponds to  $(x_i, y_j) \in [\mu]$ , then  $y_j \leq \mathbf{f}_j$  by definition of the flag  $\mathbf{f}^{\lambda/\mu}$ . Hence,  $T_{x_i, y_j} \leq \mathbf{f}_j$ .

Lastly, we will show  $\phi$  is a bijection by constructing its inverse. Let  $T \in \mathcal{F}(\mu, \mathbf{f}^{\lambda/\mu})$  and let  $D = \psi(T)$  where  $D = \{(x + T_{x,y}, y + T_{x,y}) | (x, y) \in [\mu]\}$ . Now we want to show that our new map  $\psi$  is well-defined. Notice that  $D \subseteq [\lambda]$  from the definition of the flag  $\mathbf{f}^{\lambda/\mu}$ . We want to prove that  $D \in \varepsilon(\lambda/\mu)$  by inducting on the number of flagged moves,  $\alpha'_{x,y}(\cdot)$ . Notice that  $\psi(T_\mu) = [\mu] \in \varepsilon(\lambda/\mu)$ . Suppose that for  $T \in \mathcal{F}(\mu, \mathbf{f}^{\lambda/\mu})$ ,  $D = \psi(T) \in \varepsilon(\lambda/\mu)$  and  $T' = \alpha'_{x,y}(T)$  for some active cell  $(x, y) \in T$ . Notice that the replacement of  $T_{x,y}$  with  $T_{x,y} + 1$  resulting a flagged tableau  $T' \in \mathcal{F}(\mu, \mathbf{f}^{\lambda/\mu})$  is equivalent to the cell  $(x + T_{x,y}, y + T_{x,y}) \in D$  being active. Since  $\psi(T') = \alpha_{i_x, i_y}(D)$  and  $\alpha_{i_x, i_y}(D)$  is an excited diagram, we have constructed  $\psi = \phi^{-1}$ .  $\square$

**Example 5.2.7.** Let  $\lambda = (12, 12, 10, 9, 9, 6, 6, 6)$ ,  $\mu = (7, 5, 5, 4, 2)$ , and refer to the image below. For each row  $i$  of  $\mu$  we record as  $f_i$  the row of  $\lambda$  in which the last cell of row  $i$  of  $\mu$  ended after a sequence of all possible excited moves. Thus, we have the flag  $f^{\lambda/\mu} = (3, 5, 5, 6, 8)$ .

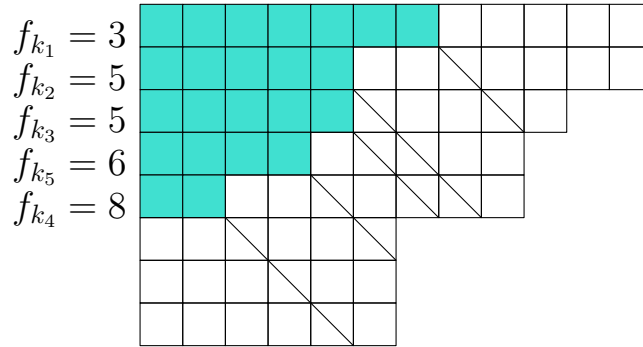


Figure 5.2. Finding the flag of the tableau of shape  $(12, 12, 10, 9, 9, 6, 6, 6)/(7, 5, 5, 4, 2)$ .

**Example 5.2.8.** Now we give an example of the map  $\phi$ . For a blue cell  $(i, j)$  in the image below, its value is  $j$  in  $T$ . If we perform reverse excited moves, that is, determine its original location, this tells the row location of  $x_i$  in the tableau.

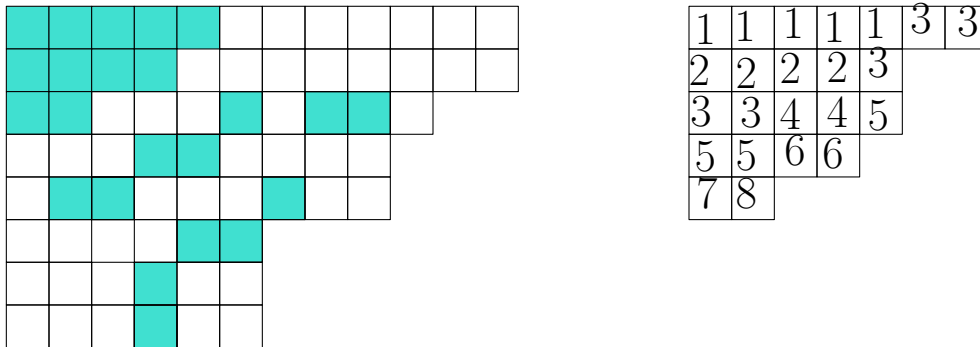


Figure 5.3. Constructing a flagged tableau given an excited diagram.

These two propositions combine to give the following corollary:

**Corollary 5.2.9** ([10], Corollary 3.7). *Let  $\lambda$  and  $\mu$  be partitions such that  $\mu \subset \lambda$  and  $\mathbf{f}^{\lambda/\mu}$  be as in Definition 5.2.5. Then*

$$e(\lambda/\mu) = \det \left[ \left( \begin{array}{ccc} \mathbf{f}_i + \mu_i - i + j - 1 & & \\ & \mathbf{f}_i - 1 & \\ & & \end{array} \right) \right]_{i,j=1}^{\ell(\mu)}.$$

In order to prove Corollary 5.2.2, we require a result that counts the number of non-intersecting lattice paths. This result was predicted by Lindström, but stated by Gessel and Viennot [20]. The statement of the lemma depends on the following definitions.

**Definition 5.2.10** ([20]). Let  $A = \{a_1, \dots, a_n\}$  be a collection of starting points and  $B = \{b_1, \dots, b_n\}$  be a collection of ending points in the two-dimensional lattice. A *lattice path* from  $a_i$  to  $b_j$  is a sequence of north steps,  $(0, 1)$ , and east steps  $(1, 0)$  beginning at point  $a_i$  and ending at point  $b_j$ . Let us denote the number of lattice paths from  $a_i$  to  $b_j$  as  $p_{ij}$ . An  $n$ -tuple of non-intersecting lattice paths from  $A$  to  $B$  are paths  $(P_1, \dots, P_n)$  such that for all  $i \neq j$ ,  $P_i$  and  $P_j$  have no point in common. For clarity of notation, we define a matrix

$$M = \begin{bmatrix} p_{11} & p_{12} & \cdots & p_{1n} \\ p_{21} & p_{22} & \cdots & p_{2n} \\ \vdots & \vdots & \ddots & \vdots \\ p_{n1} & p_{n2} & \cdots & p_{nn} \end{bmatrix}.$$

The lemma below states  $\det(M)$  is the number of non-intersecting lattice paths from  $A$  to  $B$ .

**Lemma 5.2.11** (Lindström, Gessel-Viennot Lemma, [4]). *Using the notation established in the previous definition, we have that the number of tuples  $(P_1, \dots, P_n)$  of non-intersecting lattice paths is given by  $\det(M)$ .*

Below is a definition of a type of non-intersecting lattice paths for Young diagrams of staircase shape.

**Definition 5.2.12** ([11]). A *border strip* of  $[\lambda]$  is a connected skew shape without any  $2 \times 2$  squares. The starting point of the strip is located at a southwest cell from the endpoint. An *outer border*



*strip* is the strip from the most southwest cell of  $[\lambda]$  to the most northeast cell which contains all the cells that share a vertex with the outside corners. The *Lascoux-Pragacz decomposition* of  $\lambda/\mu$  decomposes  $[\lambda/\mu]$  into  $k$ -maximal outer border strips by using the following process:

1. Let  $\theta_1$  be the outer border strip of  $[\lambda]$ .
2. Let  $\theta_2$  be the outer border strip of  $[\lambda] \setminus \theta_1$ .
3. Continue defining each  $\theta_j$  as the outer border strip of  $[\lambda] \setminus \theta_{j-1}$  until an outer border strip intersects  $[\mu]$ .
4. Once  $[\mu]$  begins to be intersected, decompose the remaining smaller connected components.

We refer to  $\theta_1$  as the *cutting strip* and denote it as  $\tau$ . For  $p, q \in \mathbb{Z}$ , we write the substrip of the cutting strip from  $p$  to  $q$  as  $\varphi[p, q]$ . We say that  $\varphi[p, p] = (1)$ ,  $\varphi[p + 1, p] = \emptyset$ , and for  $p > q + 1$ ,  $\varphi[p, q]$  is undefined. Let  $p(\theta_i)$  and  $q(\theta_i)$  be the contents of the starting and ending point of the strip  $\theta_i$ . Then we define the strip  $\theta_i \# \theta_j$  as the substrip  $\varphi[p(\theta_j), q(\theta_i)]$  of  $\tau$ .

**Example 5.2.13.** In the example for  $\delta_8/\delta_4$  below, we see the  $\theta_1$  and  $\theta_2$  are border strips. Notice the cutting strip  $\theta_1$  connects outside corners.

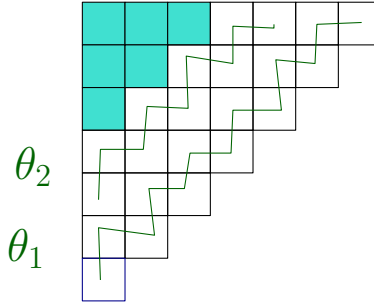


Figure 5.4. Border strips of  $\delta_8/\delta_4$ .

**Theorem 5.2.14** ([7]). *If  $(\theta_1, \dots, \theta_k)$  is the Lascoux-Pragacz decomposition of  $[\lambda/\mu]$  into  $k$  maximal outer border strips, then*

$$e(\lambda/\mu) = \det [e(\theta_i \# \theta_j)]_{i,j=1}^k,$$

where  $e(\emptyset) = 1$ , and whenever  $\varphi[p, q]$  is undefined,  $e(\varphi[p, q]) = 0$ .

We give another definition of a type of non-intersecting lattice paths for Young diagrams of staircase shape.

**Definition 5.2.15.** Consider  $\delta_{n+2k}/\delta_n$ . We define a tuple of border strips strip  $(\gamma_1^*, \dots, \gamma_k^*)$ , called the *Kreiman decomposition* of  $\delta_{n+2k}/\delta_n$ , by the following process:

- Let  $\gamma_1^*$  be the border strip that begins at cell  $(n + 2k - 1, 1)$  and ends at cell  $(1, n + 2k - 1)$  which contains the cells that are below inside corners of the skew shape.
- Let  $\gamma_2^*$  be the border strip that begins at cell  $(n + 2k - 2, 2)$  and ends at cell  $(2, n + 2k - 2)$  which contains the cells below  $\gamma_1^*$ .
- Continue defining each  $\gamma_i^*$  as the inner border strip until there are  $k$  border strips.

The *support* of  $(\gamma_1^*, \dots, \gamma_k^*)$  is the set of boxes in the paths  $(\gamma_1^*, \dots, \gamma_k^*)$ . Now we let  $\mathcal{NI}(\delta_{n+2k}/\delta_n)$  denote the Kreiman decomposition of  $\delta_{n+2k}/\delta_n$ .

**Example 5.2.16.** In the figure given below, we observe the Kreiman decomposition for  $\delta_8/\delta_4$ .

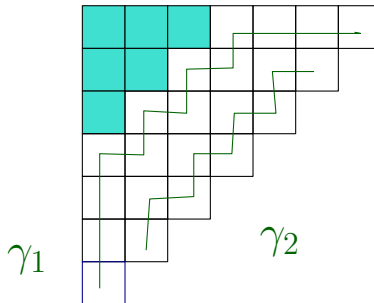


Figure 5.5. The Kreiman decomposition for  $\delta_8/\delta_4$ .

In [7], Kreiman proved that the supports of the paths in  $\mathcal{NI}(\lambda/\mu)$  are precisely the complements of  $\varepsilon(\lambda/\mu)$ .

**Proposition 5.2.17** ([7]). *The  $k$ -tuples of paths in  $\mathcal{NI}(\lambda/\mu)$  are uniquely determined by their supports in  $[\lambda]$ . Moreover, the supports are exactly the complements of excited diagrams of  $[\lambda/\mu]$ .*

Now we return to the proof of Corollary 5.2.2 from [11].

*Proof of Corollary 5.2.2.* We first prove the case where  $k = 1$ . In this case, we have  $\delta_{n+2}/\delta_n$ , the zigzag outer border strip. From Proposition 5.2.6, we know that the complement of excited diagrams of  $\delta_{n+2}/\delta_n$  are the paths  $\gamma: (n+1, 1) \rightarrow (1, n+1)$ ,  $\gamma \subseteq \delta_{n+2}$ . A rotation of these paths by  $-\frac{\pi}{4}$  radians gives us Dyck paths of length  $2n$ . Hence,  $e(\delta_{n+2}/\delta_n) = C_n$ .

Now we consider the general case for  $k$ . Then  $\delta_{n+2k}/\delta_n$  has the Lascoux-Pragacz decomposition into  $k$  maximal border strips  $(\theta_1, \dots, \theta_k)$ . Theorem 5.2.14 implies that

$$e(\delta_{n+2k}/\delta_n) = \det [e(\theta_i \# \theta_j)]_{i,j=1}^k.$$

Recall that the cutting strip of  $\delta_{n+2k}/\delta_n$  is  $\tau = \theta_1$ . The strips  $\theta_i \# \theta_j$  that are in the determinant are also zigzags, since they are substrips of  $\tau$ . The strip  $\theta_i \# \theta_j \in \theta_1$  are cells with content from  $2 + 2j - n - 2k$  to  $n + 2k - 2i - 2$ . Thus, the strip is a zigzag  $\delta_{m+2}/\delta_m$  of size  $2m + 1$ , where  $m = n + 2k + i + j + 2$ . From the above case, we know that  $\delta_{m+2}/\delta_m$  is counted by  $C_m$ . Hence,

$$e(\delta_{n+2k}/\delta_n) = \det [C_{n+2k-i-j-2}]_{i,j=1}^k = \det [C_{n+i+j-2}]_{i,j=1}^k.$$

The last equality above results from a relabeling of the matrix. Hence, the first equality of (5.1) is proved.

In order to prove the second equality of (5.1), we use the characterization of excited diagrams as flagged tableaux. Recall Proposition 5.2.6. Then we have that  $\varepsilon(\delta_{n+2k}/\delta_n)$  is in bijection with flagged tableaux of shape  $\delta_n$  with flag  $(k+1, k+2, \dots, k+n-1)$ . When we subtract  $i$  from all cells in row  $i$ , the resulting tableaux are equivalent to reverse plane partitions in  $\text{RPP}(\delta_n)$  having entries at most  $k$ . These are enumerated by the product formula due to [17].  $\square$

**Example 5.2.18.** Let  $k = 1$ . In this case, the remaining strip of  $\delta_{n+2}/\delta_n$  is the zigzag border strip. A rotation of the border strip by  $-\frac{\pi}{4}$  radians reveals that the shape is merely a Dyck path. In Proposition 5.1.2, we saw that Dyck paths are enumerated by  $C_n$ . Now we consider the general equalities. For the first equality, we begin with a skew Young diagram of shape  $\delta_{n+2k}/\delta_n$ . Then we

create border strips, not necessarily of zigzag shape. To do so, we pick the most southeast cell and create a path to the most northeast cell by going through the corner cells. The first image below is of the border strips of  $\delta_8/\delta_4$  when no excited moves have been performed. The second image is of border strips of  $\delta_8/\delta_4$  when two excited moves have occurred and the third is after three excited moves have been done.

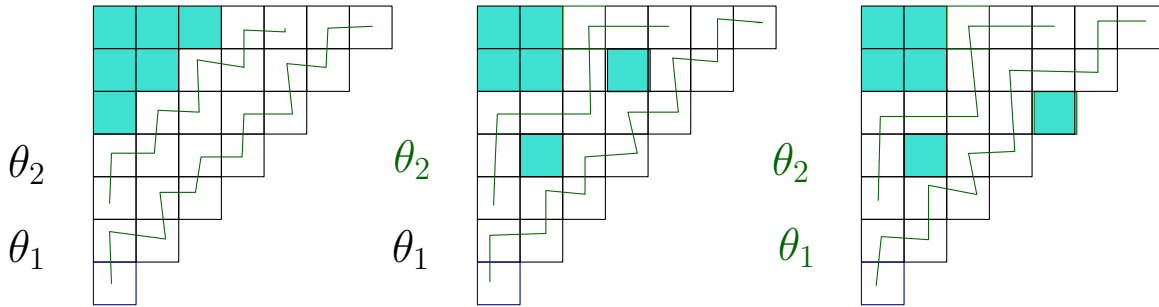


Figure 5.6. Boarder strips of  $\delta_8/\delta_4$ .

We change these to Kreiman outer decompositions by instead picking the most southwest cell and moving to the most northeast cell by going on the most northerly path. These paths are also Dyck paths. We obtain more Dyck paths by completing excited moves. The first image shows the Kreiman outer decomposition of  $\delta_8/\delta_4$  when no excited moves have been done. The second image depicts the Kreiman outer decomposition after two excited moves and the third image is after three excited moves.

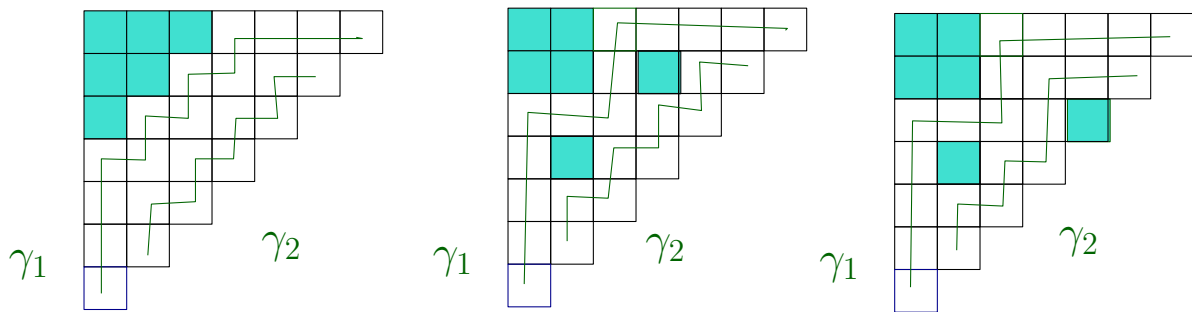


Figure 5.7. Kreiman outer decompositions of  $\delta_8/\delta_4$ .

Notice that these paths will never intersect and are actually a type of lattice path. Thus, we

can apply Lemma 5.2.11. Hence we arrive at a determinant. Since the case of  $k = 1$  established these paths are counted by  $C_n$ , we get the desired result. For the second equality, we observe that  $\varepsilon(\delta_{n+2k}/\delta_n)$  is in bijection with flagged tableaux of shape  $\delta_n$  with flag  $\mathbf{f}^{\delta_{n+2k}/\delta_n} = (k + 1, k + 2, \dots, k + n - 1)$ . If we subtract  $i$  from each  $i$ -th row, the result is equivalent to reverse plane partitions of shape  $\delta_n$  and have entries less than or equal to  $k$ . To conclude this example we find the number of excited diagrams of shape  $\delta_8/\delta_4$  as shown below:

$$\det \begin{bmatrix} C_6 & C_5 \\ C_5 & C_4 \end{bmatrix} = C_6 C_4 - C_5^2 = (132)(14) - (42)^2 = 84.$$

Applying Proposition 5.2.6 to Corollary 5.2.2, yields the following corollary.

**Corollary 5.2.19** ([11], Corollary 8.3).

$$\det \left[ \binom{n-i+j}{i} \right]_{i,j=1}^{n-1} = C_n.$$

*Proof.* From Corollary 5.2.2, we have  $|\varepsilon(\delta_{n+2}/\delta_n)| = C_n$ . Now we use Proposition 5.2.9 for  $\delta_{n+2}/\delta_n$  with flag  $\mathbf{f}^{\delta_{n+2}/\delta_n} = (2, 3, \dots, n)$ . Then we have that  $|\varepsilon(\delta_{n+2}/\delta_n)|$  is found by the determinant above. □

## 6. OTHER RESULTS

Amongst the many additional topics covered in the series of papers by Morales, Pak, and Panova [10, 11, 12] are results on Lozenge tilings and excited diagrams. In this chapter, we discuss some these results as well as some subsequent work of other authors.

### 6.1. Lozenge Tilings and Excited Diagrams

Another visual interpretation of an excited diagrams is as a lozenge tiling.

**Definition 6.1.1** ([12]). Consider a triangular grid in the plane where two of the axes are identified as  $x$  and  $y$ , as denoted below. Adjacent triangles that are paired are called *lozenges*. When a lozenge's long axis is horizontal, we call it a *horizontal lozenge*. In the image below, we have the triangular grid and three possible lozenges (the horizontal lozenge shown in green). The *local weight* is denoted  $\text{wt}(T) := \prod_{(i,j) \in \mathbf{hl}(T)} (x_i - y_i)$ , where  $T$  is a tiling of a grid and  $\mathbf{hl}(T)$  is the set of horizontal lozenges. That is, the weight of each of the horizontal lozenges is assigned by its position with respect to the  $x$  and  $y$  axes. Given a partition  $\mu$  and  $d \in \mathbb{Z}$ , consider the plane partitions of base  $\mu$  and height no larger than  $d$ . This corresponds to the region  $\Omega_{\mu,d}$  in the plane with lower side determined by  $\mu$  and the remaining side bounded by the top four sides of a hexagon of vertical side length  $d$ . Suppose  $\lambda/\mu$  is a skew partition. Then  $\Omega_{\mu}(\lambda) \subseteq \Omega_{\mu,d}$ , for  $d = \ell(\lambda) - \ell(\mu)$ , and on each vertical diagonal  $i - j = k$ , there are no horizontal lozenges with coordinates  $(i, i - k)$  when  $i - k > \lambda_i$ . Let  $D \in \varepsilon(\lambda/\mu)$ ; we define the map  $\tau(D) := T$  to be a tiling of  $T$  with base  $\mu$  such that if cell  $(i, j) \in D$ , then  $T$  has a horizontal lozenge in position  $(i, j)$  with coordinates

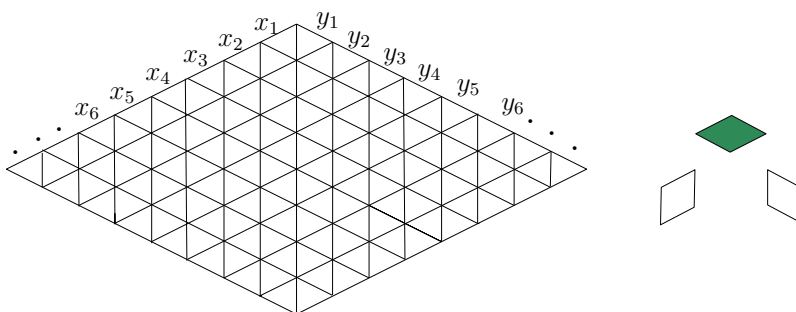


Figure 6.1. A triangular grid and lozenges.

$$(\lambda_i - i + 1, -\lambda'_j + j).$$

Now we discuss a map between excited diagrams and lozenge tilings of base  $\mu$ . Given  $D \in \varepsilon(\lambda/\mu)$ , define  $\tau(D) := T$  to be a tiling  $T$  with base  $\mu$ , such that for box  $(i, j) \in D$ ,  $T$  has a horizontal lozenge in position  $(i, j)$  as described above.

**Theorem 6.1.2** ([12], Theorem 7.2). *The map  $\tau$  is a bijection between excited diagrams  $\varepsilon(\lambda/\mu)$  and lozenge tilings  $\Omega_\mu(\lambda)$ .*

*Proof.* [12] Consider the excited diagram  $D$  as a plane partition  $P$  of shape  $\mu$  with non-positive entries using the map determined by  $P_{i,j} = -r_{i,j} + i$ , where  $r_{i,j}$  is the row number of the final position of the box  $(i, j)$  of  $\mu$  after it has been moved under the excited moves from  $\mu$  to  $D$ . Now  $P$  corresponds to a lozenge tiling by the following: set level 0 to be the top  $z$ -plane and the horizontal lozenges are moved down to the heights given by  $P_{i,j}$ . Notice that the boxes on the diagonal  $i - j = k$  cannot be moved further than the intersection of the diagonal and  $\lambda$ , since  $D \subset [\lambda]$ . This is equivalent to the condition  $(i, j) \in \lambda$  if and only if  $j \leq \lambda_i$ .  $\square$

**Example 6.1.3** ([12]). Consider the skew shape  $(3, 3, 2)/(2, 1)$ . Then we have the following five excited diagrams:

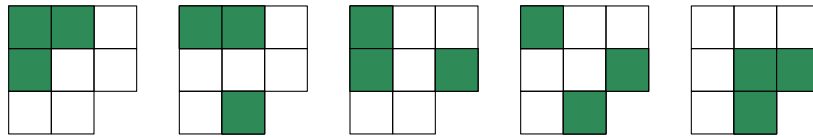


Figure 6.2. Excited diagrams of skew shape  $(3, 3, 2)/(2, 1)$ .

The lozenge tilings in  $\Omega_{2,1}(3, 3, 2)$  that correspond to the excited diagrams are:

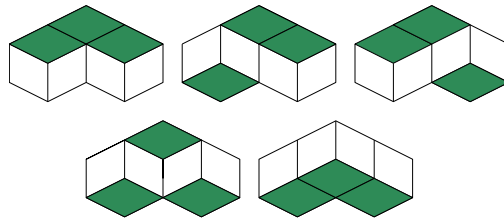


Figure 6.3. Lozenge tilings corresponding to the excited diagrams of skew shape  $(3, 3, 2)/(2, 1)$ .

## 6.2. Reverse Plane Partitions of Skew Staircase Shapes and $q$ -Euler Numbers

The paper [6] proved two conjectures stated in [11]. Before we state the conjectures, we need the following proposition. Also, recall the Euler number,  $E_n$ , is the number of alternating permutations of  $S_n$ .

**Proposition 6.2.1** ([20], Proposition 1.6.1). *The generating function for  $E_n$  is given by the following:*

$$\sum_{n \geq 0} E_n \frac{x^n}{n!} = \sec x + \tan x.$$

From [11], we have two standard  $q$ -analogues given as

$$E_n(q) := \sum_{\sigma \in \text{Alt}(n)} q^{\text{maj}(\sigma^{-1})} \text{ and } E_n^*(q) := \sum_{\sigma \in \text{Alt}(n)} q^{\text{maj}(\sigma_k^{-1})}$$

**Definition 6.2.2** ([1]). For a given Dyck path, we say it has a *high peak* when there is an upstep immediately followed by a downstep. We call the number of Dyck paths of size  $n$  with  $k - 1$  high peaks the *Narayana number*,  $N(n, k)$ .

**Remark 6.2.3.** *It is known that  $N(n, k) = \frac{1}{n} \binom{n}{k} \binom{n}{n-1}$ .*

**Definition 6.2.4** ([11]). Let the number of lattice paths from  $(0, 0)$  to  $(2n, 0)$  using the steps  $(1, 1)$ ,  $(1, -1)$ , and  $(2, 0)$  that never go below the  $x$ -axis and have no steps  $(2, 0)$  on the  $x$ -axis be called the *Schröder number*. We write the  $n$ -th Schröder number as  $s_n$ .

**Proposition 6.2.5** ([22]). *The  $n$ -th Schröder number is*

$$s_n = \sum_{k=1}^n N(n, k) 2^{k-1}.$$

The following two theorems were stated as conjectures in [11] are proven in [6].

**Theorem 6.2.6** ([6, 11]). *We have that  $p(\delta_{n+4}/\delta_n) = 2^{2n+5}(s_n s_{n+2} - s_{n+1}^2)$ . In general, for all  $k \geq 1$ , we have*

$$p(\delta_{n+2k}/\delta_n) = 2^{\binom{k}{2}} \det[s_{n-2+i+j}]_{i,j=1}^k \text{ for } s_n = 2^{n+2} s_{n-1}.$$



**Theorem 6.2.7** ([6, 11]).

$$\sum_{\pi \in RPP(\delta_{n+2k}/\delta_n)} q^{|\pi|} = q^{-N} \det[e_{2(n+i+j)-3}^*(q)]_{i,j=1}^k,$$

where  $N = k(k-1)(6n+8k-1)/6$  and  $e_k^*(q) = E_k^*(q)/((1-q) \cdots (1-q^k))$ .

### 6.3. Future Investigation

Since the HLF has an adaptation for SSYT, it is natural to want to know if there is a Hook Content Formula type adaptation for the NHLF. Other desires by the community are to find a probabilistic style bijective proof of the NHLF similar to that of [15]. Also, there is a curiosity to see how  $E_n^*(q)$  meshes into known work on multivariate Euler polynomials and statistics on alternating permutations.

## REFERENCES

- [1] E. Deutsch, An involution on Dyck paths and its consequences, *Discrete Math.* **204** (1999), 163-166.
- [2] W. Fulton, *Young tableaux*. Cambridge University Press, 1997.
- [3] J. S. Frame, G. de B. Robinson, R. M. Thrall, The hook graphs of the symmetric group, *Canad. J. Math.* **6** (1954), 316-324.
- [4] I. M. Gessel and X. G. Viennot, Determinants, paths, and plane partitions, (preprint).
- [5] A. P. Hillman and R. M. Grassl, Reverse plane partitions and tableau hook formulas, *J. Combin. Theory Ser. A* **21** (1976), 216-221.
- [6] B.-W. Hwang, J. S. Kim, M. Yoo, and S.-M. Yun, Reverse plane partitions of skew staircase shapes and  $q$ -Euler numbers. *J. Combin. Theory Ser. A* **168** (2019), 120-163.
- [7] V. Kreiman, Schubert classes in the equivariant K-theory and equivariant cohomology of the Lagrangian Grassmannian, arXiv:math.AG/0512204.
- [8] A. Lascoux and P. Pragacz, Ribbon Schur functions, *European J. Combin.* **9** (1988), 561-574.
- [9] M. E. Mays and J. Wojciechowski, A determinant property of Catalan numbers, *SIAM J. Discrete Math.*, **211** (2000), 125-133.
- [10] A. H. Morales, I. Pak, G. Panova, Hook formulas for skew shapes I.  $q$ -analogues and bijections. *J. Combin. Theory Ser. A* **154** (2018), 350-405.
- [11] A. H. Morales, I. Pak, G. Panova, Hook formulas for skew shapes II. Combinatorial proofs and enumerative applications. *SIAM J. Discrete Math.* **31** (2017), 1953-1989.
- [12] A. H. Morales, I. Pak, G. Panova, Hook formulas for skew shapes III. Multivariate and product formulas, arXiv:1707.00931.

- [13] A. H. Morales, I. Pak, G. Panova, Asymptotics for the number of standard Young tableaux of skew shape. *European J. Combin.* **70** (2018), 26-49.
- [14] H. Naruse, Schubert calculus and hook formula. Talk slides at *73rd Sé. Lothar. Combin.*, Strobl, Austria, 2014; available at [tinyurl.com/z6paqzu](http://tinyurl.com/z6paqzu).
- [15] J.-C. Novelli, I. Pak, A. V. Stoyanovskii, A direct bijective proof of the hook-length formula, *Discrete Math. Theor. Comput. Sci.* **1** (1997), 53-67.
- [16] I. Pak, Hook length formula and geometric combinatorics. *Sém. Lothar. Combin.* **46** (2001), Art. B46f, 13 pp.
- [17] R. A. Proctor, New symmetric plane partitions identities from invariant theory work of De Concini and Procesi, *European J. Combin.* **11** (1990), 289-300.
- [18] A. Ram, A Frobenius formula for the characters of the Hecke algebras, *Inventiones mathematicae* **106** (1991), 461-488.
- [19] R. P. Stanley, *Catalan Numbers*. Cambridge University Press, 2015.
- [20] R. P. Stanley, *Enumerative combinatorics*, vol. 1 (second edition), Cambridge University Press, 2012.
- [21] R. P. Stanley, *Enumerative combinatorics*, vol. 2, Cambridge University Press, 1999.
- [22] R. A. Sulanke, The Narayana distribution, *J. Statist. Plann. Inference* **101** (2002), 311-326.
- [23] G. Viennot, Une forme géométrique de la correspondance de Robinson-Schensted, in *Lecture Notes Mathematics*. **579**, Springer, Berlin, 1977, 29-58.
- [24] M. Wachs, Flagged Schur functions, Schubert polynomials, and symmetrizing operators, *J. Combin. Theory Ser. A* **40** (1985), 276-289.
- [25] D. E. White, Some connections between the Littlewood-Richardson rule and the construction of Schensted, *J. Combin. Theory Ser. A* **30** (1980), 237-247.